# Relationship between Localized Spine Deformation and Cervical Vertebral Motions for Low Speed Rear Impacts Using Human Volunteers

**Koshiro Ono*, Satoshi Inami**, Koji Kaneoka***, Tukasa Gotou***
**Yoshikatu Kisanuki****, Shigeru Sakuma****, and Kazuo Miki****
***Japan Automobile Research Institute, **University of Tsukuba**
****Tokyo Kosei-Nekin Hospital, ****Toyota Central R&D Labs., Inc.**

## ABSTRACT

It is important to more clearly identify the relationship among the ramping-up motion, straightening of the whole spine, and cervical vertebrae motion in order to clarify minor neck injury mechanism. The aim of the current study is to verify the influence of the change of the spine configuration on human cervical vertebral motion and on head/neck/torso kinematics under low speed rear-end impacts. Seven healthy human volunteers participated in the experiment under the supervision of an ethics committee. Each subject sat on a seat mounted on a sled that glided backward on rails and simulated actual car impact acceleration. Impact speeds (4, 6, and 8 km/h), and seat stiffness (rigid and soft) without headrest were selected. During the experiment, the change of the spine configuration (measured by a newly developed spine deformation sensor with 33 paired set strain gauges and placed on the skin) and the interface load-pressure distribution was recorded. This was measured by means of a Tekscan system at a rate of 100 f/s, placed between the seat and subject. The cervical vertebrae motion was also recorded by 90 f/s cineradiography. Furthermore, analysis was made to quantify the relationship between the cervical vertebrae motion and the change of the spine configuration.

The localized straightening of the lumbar spine starts at around 30 ms with the rigid seat. The localized straightening of the thoracic spine reaches the maximum at around 80 ms when the load-pressure distribution is at its peak value due to the interaction between the shoulder and the seatback. On the other hand, for the softer seat, the pelvis starts to sink into the seat back and cushion at around 70 ms. As for such seat the load-pressure is distributed over a large area, the localized straigthening of the middle thoracic spine occurred together with deflection of seatback itself at around 120 ms. The results of this study can help clarify the relationship between the localized straightening of the spine and cervical vertebrae motion with respect to the difference in seat characteristics.

**THE HYPEREXTENSION OF NECK** was pointed out as a major factor to cause neck injuries (including whiplash) sometime ago. The authors (Ono et al. 1993, 1997-1, 1997-2, 1998, Kaneoka et al. 1998), however, identified another

factors that may lead to the neck injuries even if the hyperextension does not take place. Although the mechanism of the so-called "whiplash" has not been completely identified, phenomena observed in impact are well recognized. They can be divided into the following (Figure 1).

1) Initial Impact Response Phase: Neck is pushed up due to torso ramping-up motion and spine straightening. The occupant's spine, normally curved, starts to be pushed against the seatback, and the torso ramps up and pushes the neck upward at the same time.
2) Middle Phase - Head rapid backward motion (S-shape deformation): The head inclines rapidly backward relative to the torso, resulting in a significant retraction between the head and neck.
3) Final Phase - Head backward inclination: The neck rotates as the head inclines markedly relative to the torso.

The headrest installation was made obligatory, and the use of headrest is common because of the recognition that it is a crucial mean to reduce neck injuries in the final phase of impact. Several reports (Kahane 1992, Nygren 1984) have shown that the so-called "whiplash" injuries caused by the "hyperextension" of neck have been reduced significantly by the above. However, the question of how the occupant's motions in the initial impact phase - spine straightening in particular - influence the occurrence of neck injury have not been answered yet.

In this regard, spinal deformation and seatback load-pressure measurements have been conducted in this study. This is in addition to the low speed rear impact tests conducted on volunteers by means of cineradiography done in the past. Spinal deformation and seatback load-pressure measurements were done with the following goals:

1) to determine influences of seatback and the seat stiffness on human head/ neck/torso kinematics and on the change of spinal cofiguration.
2) To determine the influence of spine strightening on the cervical vertebrae motion.

## METHODS OF EXPERIMENTS

The test apparatus, measurement method, etc. are the same as those described in the paper presented by the authors (Ono et al. 1998). The gist of the paper and the flexible spine deformation sensor developed and introduced in the new study will be described in the following.

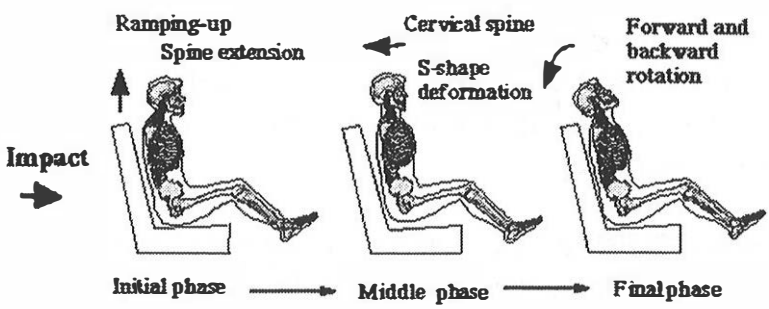


**Figure 1. Human response to rear-end impacts**

**VOLUNTEERS AND INFORMED CONSENT** - Seven adult male volunteers with average age of 24 years participated in this study. The data on subjects anthropometry are omitted here, as they were described in Davidsson's paper (1999). It was confirmed through X-ray that the subjects did not have any degenerative cervical spine. The protocol of experiments was reviewed and approved by the Tsukuba University Ethics Committee, and all volunteers submitted their informed consent in writing according to the Helsinki Declaration (WHO/CIOMS Guidline 1988).

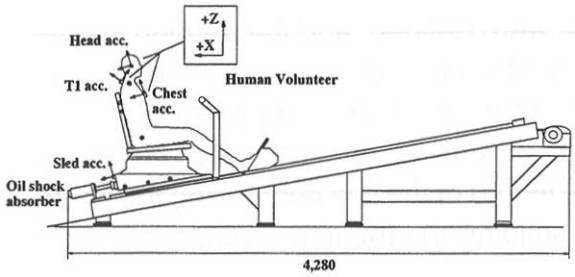


**Figure 2. Outline of sled test apparatus and the coodinate systems**

**Table 1. Measurement Items**

| Locations | | Items | Axis | Model |
|---|---|---|---|---|
| Sled | | Velocity | X | Photo sensors |
| | | Acceleration | X, Y, Z | Kyowa AS-50HA |
| Subject | Head - Upper | Acceleration | X, Z | Endevco 7264A (20G Cal.) |
| | - Lower | Acceleration | X, Z | Endevco 7264A (20G Cal.) |
| | T1 | Acceleration | X, Z | Endevco 7264A (20G Cal.) |
| | | Angular velocity | Y | Murata ENC-05E |
| | Frontal Chest | Acceleration | X, Y, Z | Kyowa AS-50HA |
| | Pelvis | Acceleration | X, Z | Endevco 63B-100 |
| | | Angular velocity | Y | Murata ENC-05E |
| | EMG | Control | Skin | |
| | | SCM(L) | Sternoclaidomastoid muscle (Left) | |
| | | PVM (L) | Paravertebral muscles (Left) | |
| | | TZ(L) | Trapezius muscles (Left) | |
| | | SCM (R) | Sternoclaidomastoid muscle (Right) | |

**SLED APPARATUS** - A sled apparatus angled at 10 degrees to simulate rear impact as shown in Figure 2 was used in the experiments. The coordinate system is also shown in Figure 2.

**CINERADIOGRAPHY** - A cineradiographic system (Cine-system: Angiorex made by Toshiba Medical Inc.) was applied to the analysis of the cervical vertebral motions in rear impact, and the template method was used to analyze the cineradiographic images.

**MEASURED ITEMS AND NECK LOAD** - The items measured on each sled test subject are shown in Table 1. Four channel accelerometers with the combination of two sets of biaxial accelerometers for X and Z axes were used in the measurement (Ono et al. 1997). The impact loads acting on the head and neck of subject were calculated based on the acceleration of the center of gravity of the head, estimated head mass and the moment of inertia.

**SUBJECT'S VISUAL MOTIONS AND SPINAL EXTENSION** - The visual motions of subject's head, neck and torso were measured as shown in Figure 3. Target marks were adhered over two accelerometers on the upper and lower portions of the head, accelerometer on the T1 and front chest, and over the skin below the auditory meatus close to the center of gravity of the subject's head, shoulder above the 12th rib, iliac crest, and upper sternum. The motions were measured with a high speed VTR camera (made by MEMORACAMERA Inc.) at the speed of 500 frames per second. The images were analyzed with ImageExpress made by NAC Inc. In the analysis, joints between the head-neck

and the neck-torso, and the head-neck link were defined, and the rotation angles of the head, neck and upper torso were determined. The spine extension was defined and analyzed as the change in the length of the line connecting the neck-torso joint and the iliac crest.

**SPINAL DEFORMATION MEASUREMENT SYSTEM** - The spinal deformation measurement system consisted of units to measure the deformations of the spine (thoracic spine, lumbar spine and sacra), and units to measure the rotation angle and displacement of pelvis (corresponding to the first sacrum) at the bottom of the spine.

The spinal deformation was measured with a tape sensor consisting of a 0.3 mm thick stainless sheet with 33 pairs of strain gauges adhered (Figure 4). The motion and the displacement of pelvis were measured with the angular gyro-sensor and accelerometer adhered near the first sacrum. Figure 5 shows the accelerometers and gyro-sensors together with the touch sensors that detect the starting time of the load-pressure on the subject. The tape sensor was attached to plaster tape used in athletics. This tape was adhered to the skin over the spine. A point over the first sacroiliac spineor was used as the reference point. A sheath made of Teflon was used over the tape, considering the variation of the length over the skin. The spinal deformation was determined as follows - the deformation of the stainless sheet was calculated using the strain measured with the tape sensor. At the same time, the values on the coordinate system at individual measuring locations on the stainless sheet were converted according to the rotation angle and the displacement measured on the pelvis. The measuring signals were sent to the

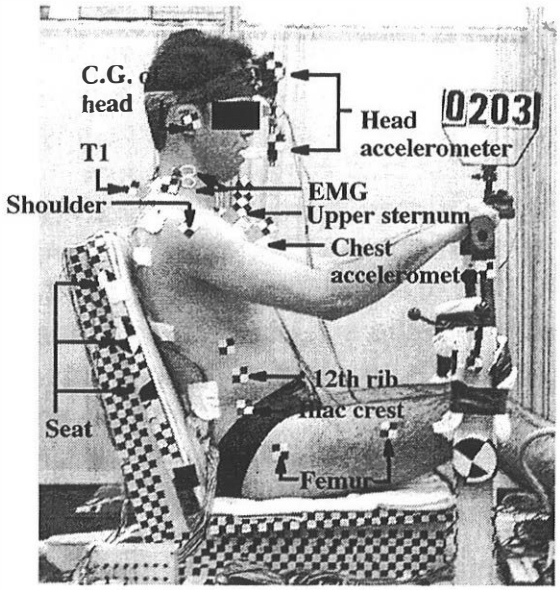


**Figure 3. Lateral view of the head/neck/torso with mounted accelerometers, EMG electrodes, targets for high speed video**

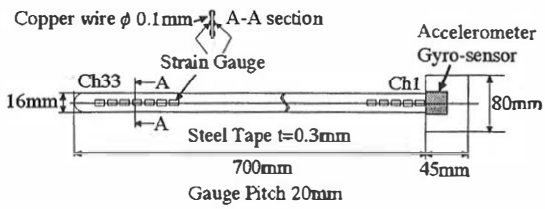


**Figure 4. Tape sensor for the spinal deformation measurement**

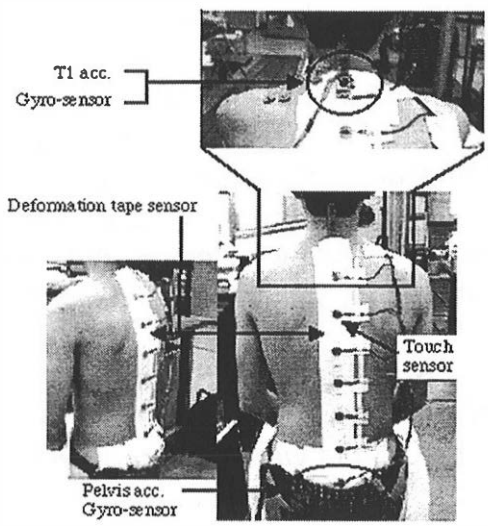


**Figure 5. Installation of deformation tape sensor, accelerometers, and gyro-sensors for volunteers**

MPU (micro processor unit) and processed by the unit (Figure 6). It was decided to name the deformation measurement system as TSDMS (Toyota Central Research & Development Spinal Deformation Measurement System).

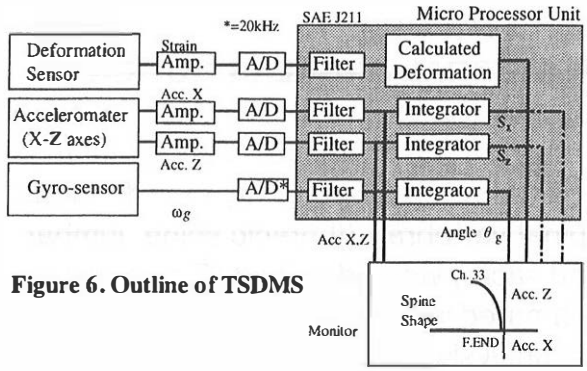


**Figure 6. Outline of TSDMS**

**ANALYSIS OF SPINAL MOTIONS** -The analytical principles are the same as those described in the paper presented by Ishiyama et al. (1994). The spinal deformation was calculated using the following equation (1): The curvature related to the strain measured at the location of each gauge was subjected to spline interpolation to obtain the equation for the curvature distribution over the entire length of sensor. Using this equation and Equation (2), (3) for the curvature in each length increment and the two-dimensional coordinate values shown in Figure 7, the coordinate value at each measured point on the stainless sheet was calculated. Then the value thus calculated was expressed in the global coordinate system set on the ground according to the rotation angle and the acceleration measured on the pelvis. By repeating this process , the spinal motions measured with the tape sensor on the two-dimensional plane were determined.

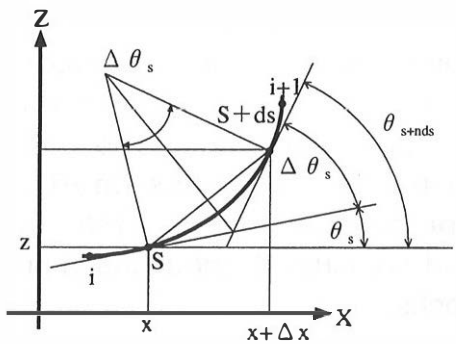


**Figure 7. Coordinates and notations**

$$\varepsilon_i = \frac{t}{2} k_i \qquad (1)$$

$\varepsilon_i$: *Strain* $\quad k_i$ : *Curvature*

$$\Delta X = ds \bullet \cos(\theta_s + \Delta\theta_s / 2) \qquad (2)$$

$$\Delta Z = ds \bullet \sin(\theta_s + \Delta\theta_s / 2) \qquad (3)$$

$ds$: *Length increment*

$\theta_s$ : *Angle* (*deg.*)

**MEASUREMENT ACCURACY** - The measurement accuracy was determined by setting the tape sensors along the circumference of a disc with a known diameter. An example of measured results is shown in Figure 8. The measured form well agreed with the shape of the disc circumference. The measurement errors were within +/- 5 % of the actual deformation.

**INTERFACE LOAD-PRESSURE DISTRIBUTION** - Tekscan system was used for the measurement of the load-pressure distribution between the subject and the seatback. The sheet mat used as the pressure sensors was BIGMAT (Nitto) 2000 type on which 2,112 sensor units were set over 44 rows and 48 columns. The size of each sensor unit was 440 mm x 480 mm. The calibration of seat mat sensors was done at TCRDL (Toyota Central Research & Development Lab.), with the measurement errors being within +/- 5 %. The data sampling interval was 10 ms.

**ANALYSIS OF SPINAL VERTEBRAL ANGULAR MOTION** - X-ray was taken with the spinal tape sensors attached to each subject, then the positions corresponding to individual spinal vertebrae (thoracic spine, lumbar and sacra) were identified (Figure 9) and compared with the spinal deformation for the analysis of changes in rotation angles of the vertebrae. Six subjects out of ten were selected in this analysis. The locations and angles of the individual vertebrae at the sitting position for the rigid seat are as shown in Table 2.

**DIVIDED INTERFACE PRESSURE SENSOR BLOCKS AND CORRESPONDENCE WITH POSITIONS OF SPINE VERTEBRAE** - Each sensor with 44 rows was divided into six blocks and averaged at the midpoint to compare the pressure pattems with the spinal deformations. The same procedure was applied to the direction of columns. The values thus obtained were assumed as the representative values of the interface load-pressure distributions in individual blocks.

**TEST MATRIX** - Both rigid seat and standard seats available in the market, without headrest (head restraint), were used in this study to find how the difference in seat stiffness at impact velocities of 4, 6 and 8 km/h would influence the cervical vertebral motions, using 10 subjects as shown in Table 3. The subjects' visual motions could not be observed by means of cineradiography.

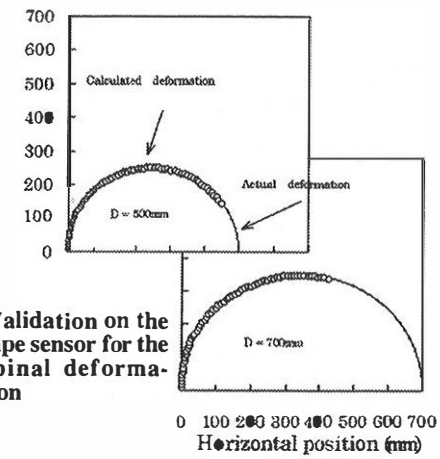


**Figure 8. Validation on the tape sensor for the spinal deformation**

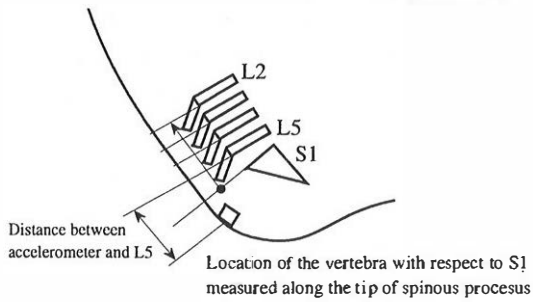


**Figure 9. Measurement of location of the vertebrae**

**Table 2. Location and Angle of the Spinal Vertebra**

| Unit | Location* | | Angle** | |
|---|---|---|---|---|
| | Ave. dist. (mm) | Std. dev. (+/- : mm) | Orientation (deg.) | Std. dev. (+/- : deg.) |
| L5 | 4 | 1 | 115 | 8 |
| L4 | 32 | 4 | 121 | 4 |
| L3 | 67 | 7 | 120 | 4 |
| L2 | 103 | 9 | 118 | 5 |
| L1 | 144 | 8 | 115 | 3 |
| T12 | 185 | 8 | 111 | 3 |
| T11 | 219 | 8 | 110 | 2 |
| T10 | 251 | 11 | 108 | 2 |
| T9 | 282 | 10 | 108 | 2 |
| T8 | 308 | 10 | 107 | 3 |
| T7 | 338 | 11 | 105 | 3 |
| T6 | 368 | 10 | 102 | 5 |
| T5 | 399 | 12 | 97 | 6 |
| T4 | 425 | 13 | 91 | 4 |
| T3 | 450 | 14 | 88 | 1 |
| T2 | 474 | 15 | 84 | 1 |
| T1 | 496 | 13 | 80 | 2 |

*: Location shows the position with respect to S1
**: Counter clockwise angle of the inferior-superior orientation from the horizontal plane

**Table 3. Test Matrix**

| | Impact velocity | Sitting position | Type of seat | Headrest |
|---|---|---|---|---|
| 7 adult males | 4<br>6 km/h<br>8 | Standard | Rigid<br><br>Standard | Without |

Therefore, both VTR experiments and cineradiography were conducted under the same conditions.

## RESULTS

The authors pointed out in a previous paper (Ono et al. 1997-1, 1997-2, 1998) that the spinal extension caused by the spine pushed against the seatback in rear impact had a great influence on the non-physiological motions of cervical vertebrae.

An example of experiment using a rigid seat without headrest tested at the impact velocity of 8 km/h is described here, focusing mainly on the seatback-subject interface load-pressure distribution and the state of spinal extension.

Figure 10 shows the variation of the seatback pressure distribution, setting the pressure to zero prior to impact. Figure 11 shows the subject's visual motions taken by a high speed video camera. Figure 12 shows the spinal deformations. The spinal deformation for each moment of impact is also shown in Figure 11. Figure 13 shows the time-histories of the loads on the neck, the accelerations of the sled and of the individual regions of the subjects, head and torso angles, and EMG. Figure 14 shows the cervical vertebral motions taken using cineradiography.

The seatback pressure started to generate at the lumbar spine around 20 ms (Fig. 10), accompanying the localized extension of lumbar. At around 80 ms, the seatback exhibited the maximum value of load-pressure. The pressure around lumbar and the upper torso also became high, with the maximum pressure distribution found around the shoulder blades. Around 70 ms, the localized extension of thoracic spine was found, and the axial compression of the neck became maximum (Fig. 12). In terms of spinal deformations, localized flexions and extensions of upper thoracic and lumbar spines were observed, with a particularly significant deformation of upper torso at the shoulder blades level. In terms of cervical vertebral motions around this region, the torso ramping-up motion increased rapidly, together with the maximum neck axial force.

The visual motions of the subject were as follows. At around 50 ms in the initial phase of impact, slight translational motions of the head and torso were observed without noticeable rotation angles of the head and torso (Fig. 13). Around the time when the neck axial force became maximum, the backward rotation of torso occurred. The maximum spine extension was found around 150 ms. At around 200 ms in the final phase of impact, the visual motions - i.e., head and torso rotation angles - became maximum with a S-shape deformation of cervical vertebrae (Fig. 14). The primal impact to the cervical vertebrae already disappeared around that time.

The results for the standard seat are as follows, though the data are not shown in the figures. The rise of head and T1 accelerations is delayed by 20 to 30 ms in comparison to the rigid seat, as the seat stiffness is lower. The subject's hips sink into the seat cushion around 70 ms, where the interface load-pressure rises while the lower cervical vertebrae start to be pushed up, and the vertebral axial compression force becomes maximum around 100 ms. The spinal extension

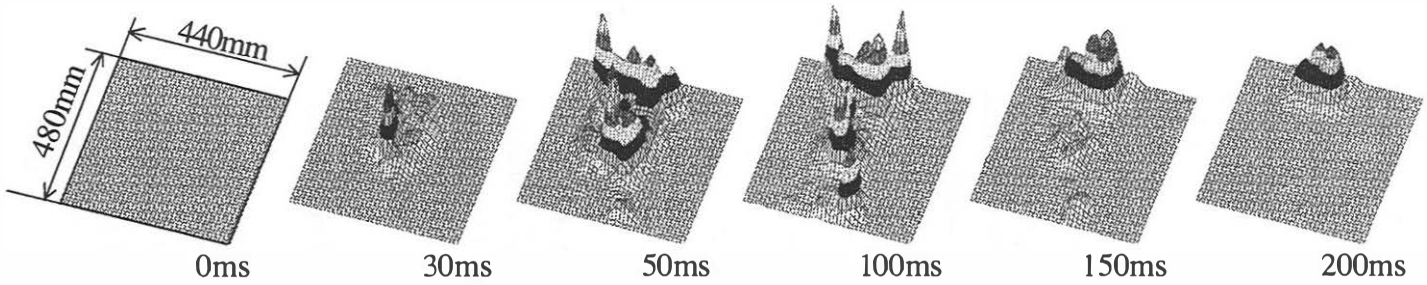


**Figure 10. Seatback load-pressure distribution by Tekscan system**

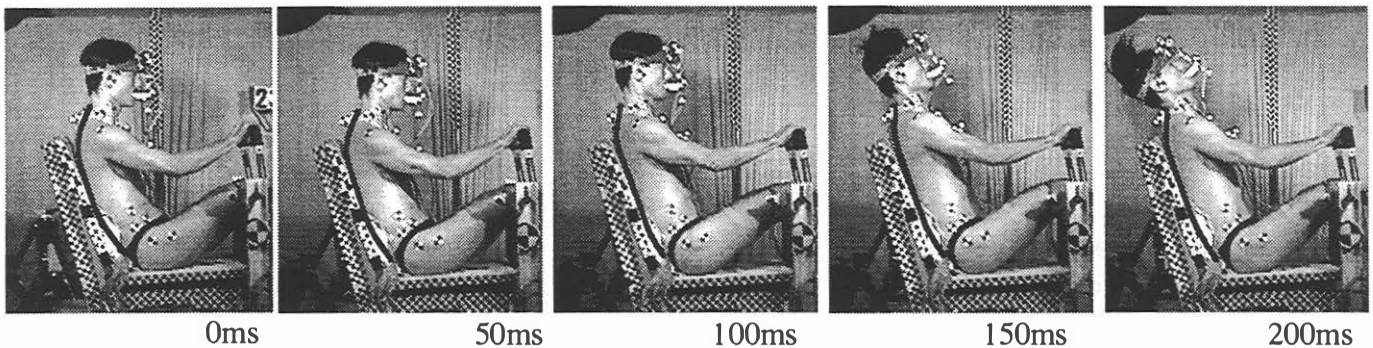


**Figure 11. Visual motion (by 500 f/s VTR) together with the spinal deformations (shown by solid line)**

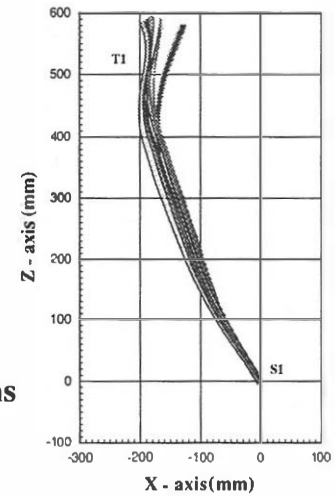


**Figure 12. Time-histories of the spinal deformations for each 10ms (Rigid seat: 8 km/h)**

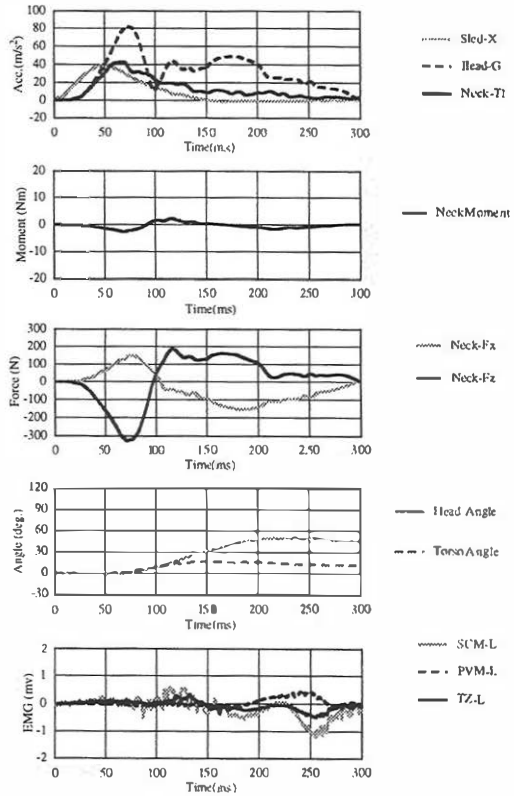


**Figure 13. Time-histories of accelerations of the sled, head, thorax, forces on neck, angles of head, torso and EMG responses on the subjects for the R-seat (8km/h)**

shows roughly maximum around 150 ms, and the entire torso sinks into the seatback. Then rebounding starts around 160 ms, and the entire configuration of spines becomes nearly straight as the upper torso extends backward and the region around the pelvis extends forward.

Variations in visual motions of head/neck/torso among the subjects are omitted here, as they are described in the paper (Davidsson, et al. 1999).

**CHANGES IN ROTATION ANGLES OF INDIVIDUAL CERVICAL VERTEBRAE** - It was found in both rigid and standard seats, despite the difference in stiffness, that the change in spinal configuration was influenced markedly by the motions of head, neck and torso - and by the cervical vertebral motion in particular. It was also found that the change in spinal configuration did not take place at once but occurred by reflecting the difference in the interaction between the seatback and the torso.

In this study, the change in spinal configuration was considered as the change in rotation angles of individual vertebral segments when studying the influence of seat stiffness. For rigid seat, Figure 15 shows the rotation angles of angular cervical vertebrae segments analyzed with cineradiography. Figure 16 shows the spinal extensions derived from the change of linear distance between the neck-torso joint and the iliac crest. Figure 17 shows the rotation angles corresponding to those of individual spinal segments - sacra, lumbar and thoracic spines - calculated from the spinal tape sensor of TSDMS. The values of the rotation angles are plotted in the figure setting the initial value to zero, with the values in (+) direction representing extensions, and those in (-) direction representing flexions. Figure 18 shows the angle of sacra, lumbar and thoracic vertebral segments relative to lower segment. Figure 19 shows the time-histories of interface load-pressure distribution where the pressure is divided into 6 blocks and the values are averaged for each block.

It is found from these figures that the lumbar vertebrae (L1-L4) flex while the thoracic spines (T4-T5) extend around 30 ms after impact on the rigid seat. The

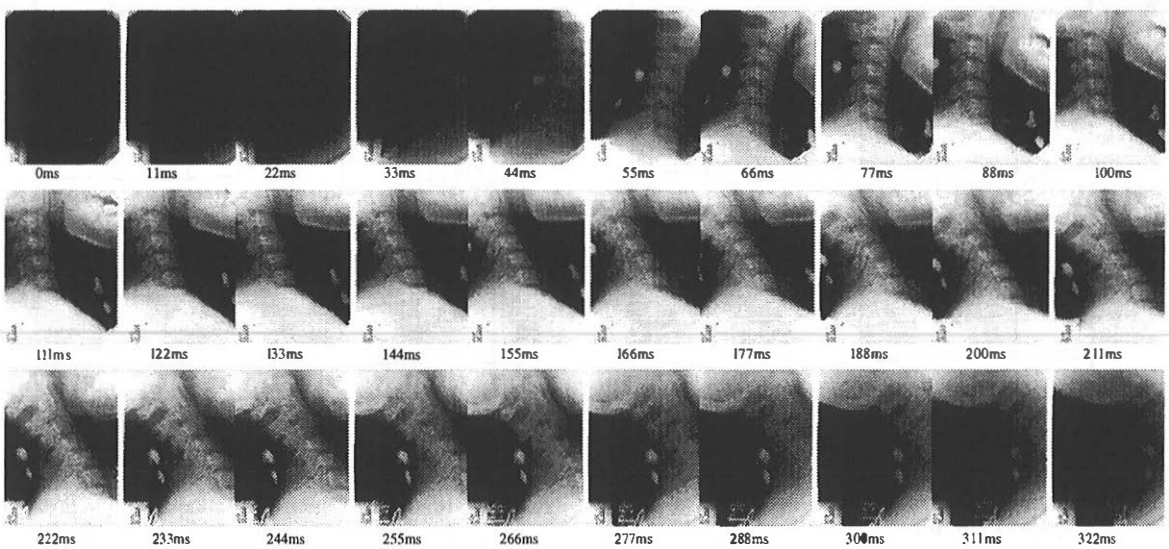


**Figure 14. Cervical vertebrae motion by X-ray cineradiography (90 f/s: Rigid seat; 8km/h)**

interface load-pressure distribution shows that region between thoracic vertebrae T11 and T12 acts as the pivot for the interaction between the subject's back and the seatback, and that lumbar vertebrae beneath the pivot travel backward together with the pelvis due to the femoral inertia caused by the impact, resulting in flexions of lumbar vertebrae (L1-L3). On the other hand, the thoracic vertebrae (T1-T5) flex on the pivotal region between T6 and T8, resulting in the backward travel of

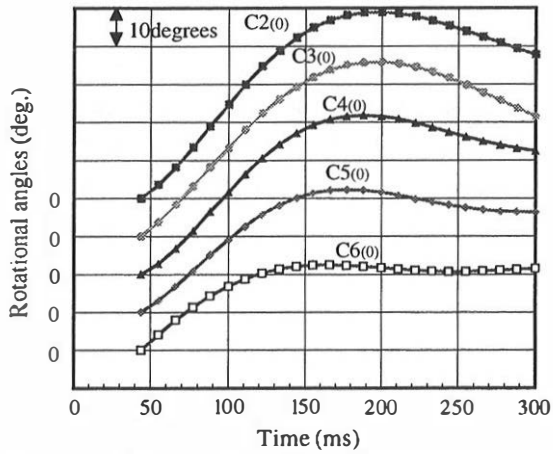


**Figure 15. Rotational angles of cervical vertebrae segments (The initial angle is set to zero and vertebrae curves are shown separately. Rigid seat; 8 km/h)**

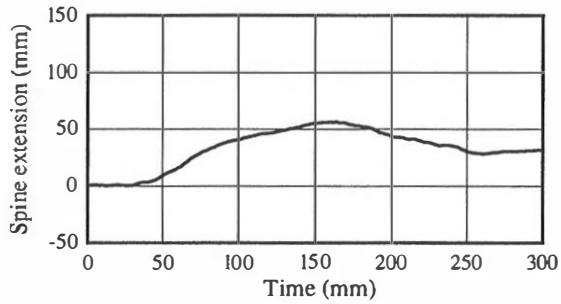


**Figure 16. Spine extension : This spine extension was analyzed as the linear distance between the neck-torso joint and each target on the iliac crest defined in the previous study [4]. (Rigid seat; 8 km/h)**

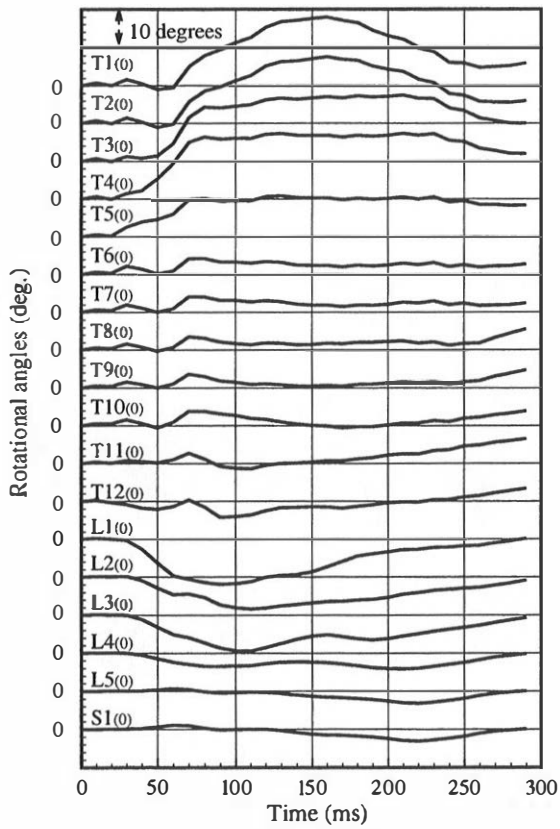


**Figure 17. Rotational angles corresponding to those of spinal segments (sacra, lumbar and thoracic spines) calculated from the TSDMS. (The initial angle is set to zero and vertebrae curves are shown separately. Rigid seat; 8 km/h)**

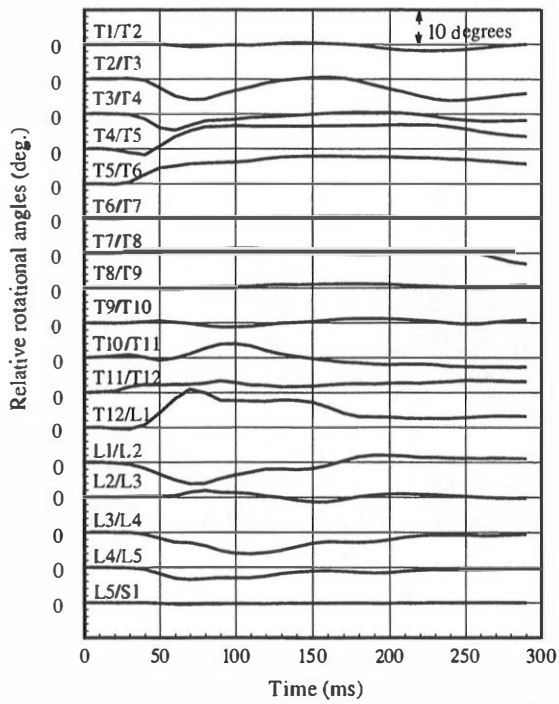


**Figure 18. Angle of spinal vertebral segments relative to lower segment. (The initial angle is set to zero and vertebrae curves are shown separately. Rigid seat; 8 km/h)**

upper torso. Around 60 ms after impact, the upper torso vertebrae - T1 in particular - extend and rotate on the pivotal region between the thoracic spines T6-T10, as the region around the shoulder blades interacts intensely with the seatback, resulting in the push-up motion and extension against the cervical vertebral lower region (C7-C6). In terms of changes in relative rotation angles of individual spine vertebrae, the rotation angles become larger for lumbar vertebrae (L4-L1) and thoracic spines (T2-T6, T10-T12). It can be said from the foregoing results that the rotation of the first thoracic spine (T1) is the direct reflection of the rotation of thoracic spine upper region (T5-T6).

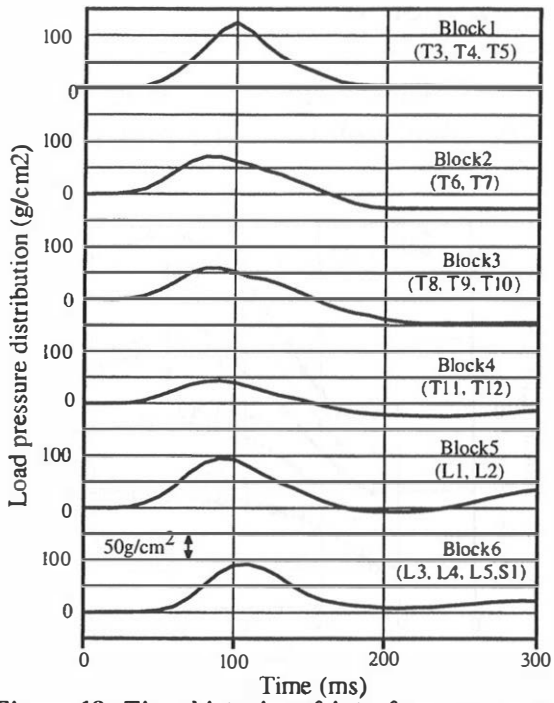


**Figure 19. Time-histories of interface pressure distribution divided into 6 blocks of sheet mat (The initial load is set to zero and curves are shown separately. Rigid seat; 8 km/h)**

For standard seat, Figure 20 shows the change in rotation angle of each vertebral segment. Figure 21 shows the spine extension derived from the change of linear distance between the neck-torso joint and the iliac crest. Figure 22 shows the calculated rotation angles which correspond to the measured rotation angles of individual sacra, lumbar and thoracic spines that occurred on the standard seat. Figure 23 shows the angle of sacra, lumbar and thoracic vertebral segments relative to lower segment. Figure 24 shows the time-histories of each divided block of interface pressure distribution.

In comparison with the rigid seat, the standard seat reveals that the lower lumbar spines (S1 to L5) and the upper thoracic spines (T1-T4) extend around 40 ms, while the upper lumbar spines (L1-L4) and the lower thoracic spines (T8-T12) flex slightly. The lower lumbar spines (S1 to L5) extend as the hips and the thighs sink into the seatback and seat cushion due to inertia, and rotate around the pivotal region of the lower lumbar spines (L4) at around 70 ms. The upper thoracic spines (T1-T5) rotate and extend backward with a region around the shoulder blades acting as the pivot. The upper lumbar spines (L1-L4) and the lower thoracic spines (T8-T12) flex slightly with a region around T7 acting as the pivot. In terms of changes in relative rotation angles of individual spine vertebrae, some motions are found in the regions of lumbar spines (L5-L2) and thoracic spines (T4-T6, T7-T8). It can be said that the rotation of T1 is the direct significant reflection of rotations of lower spinal vertebrae such as the middle thoracic and lumbar spinal vertebrae.

## DISCUSSION

**FLEXIBILITY OF SPINAL VERTEBRAE AND ACCURACY -** According to the spinal deformations and seatback interface load-pressure distributions

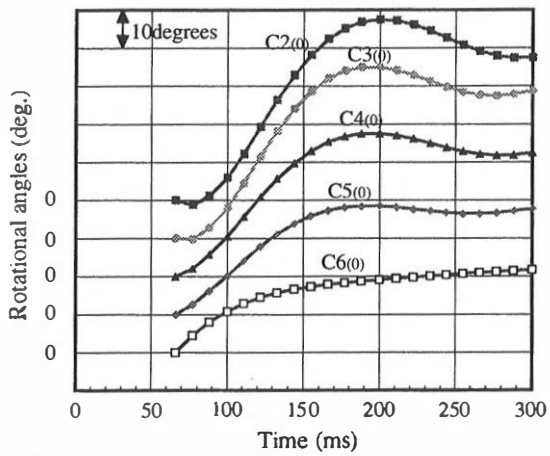


**Figure 20. Rotational angles of cervical vertebrae segments (The initial angle is set to zero and vertebrae curves are shown separately. Standard seat; 8 km/h)**

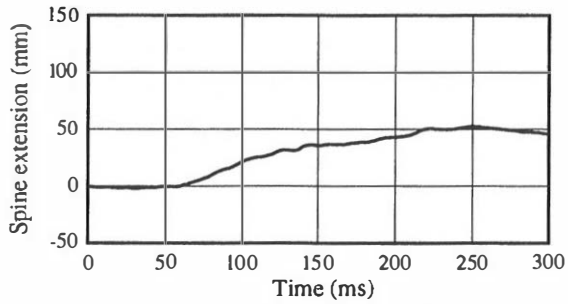


**Figure 21. Spine extension : This spine extension was analyzed as the linear distance between the neck-torso joint and each target on the iliac crest defined in the previous study[4]. (Standard seat; 8 km/h)**

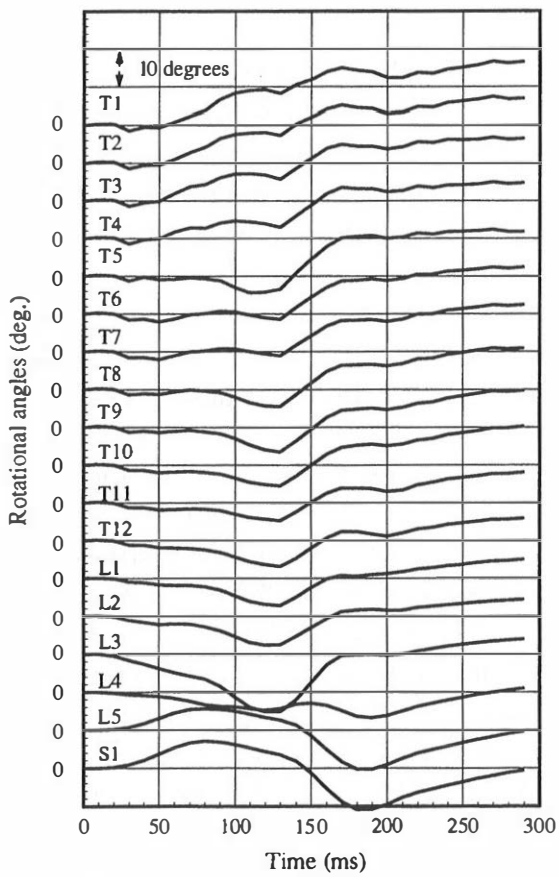


**Figure 22. Rotational angles corresponding to those of spinal segments (sacra, lumbar and thoracic spines) calculated from the TSDMS. (The initial angle is set to zero and vertebrae curves are shown separately. Standard seat; 8 km/h)**

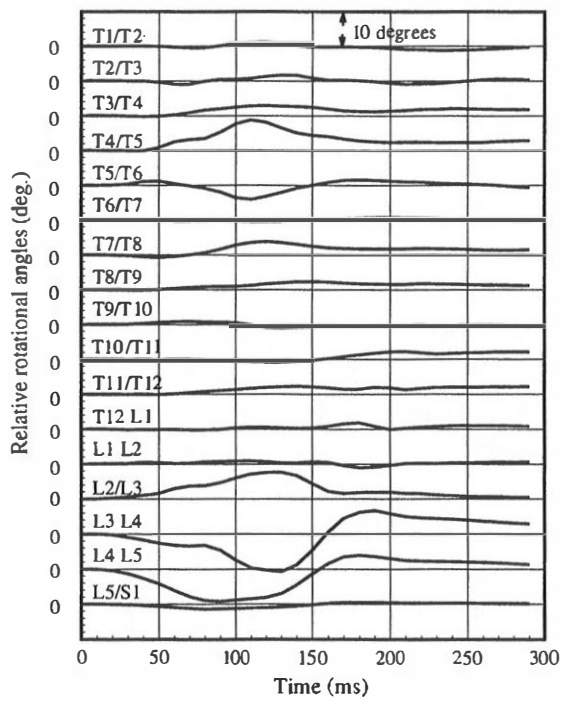


**Figure 23. Angle of spinal vertebral segments relative to lower segment. (The initial angle is set to zero and vertebrae curves are shown separately. Standard seat; 8 km/h)**

measured on each subject's skin, it is found that the relative rotational angles of individual spinal vertebrae in rear impact are large not only for lumbar spines but also for lower and upper thoracic spines (T2-T6, T10-T12), though they may vary according to the seat stiffness. No studies were available in the past regarding dynamic measurements of spinal deformation and rotation angles of individual spinal vertebrae of volunteers. In this study, the flexibility (range of motion) in rotation angles of spinal vertebrae was compared with the flexibility in static state reported by Lumsden et al. (1968), White and Panjabi (1990), and the dynamic flexibility was also studied according to the data measured and analyzed in this study. The accuracy of measured and analyzed data on the rotation angles of individual spinal vertebrae according to measurements of spinal deformations was also clarified. It was done by installing the tape sensors onto each subject and conducting X-ray under both standing and sitting positions of the subject. Then each spinal vertebral location defined by the tape sensor and the motion of each spinal vertebra at the sitting and standing positions were compared, and the error was approximately +/- 5 %. However, cineradiography in dynamic conditions could not be done, which calls for further studies.

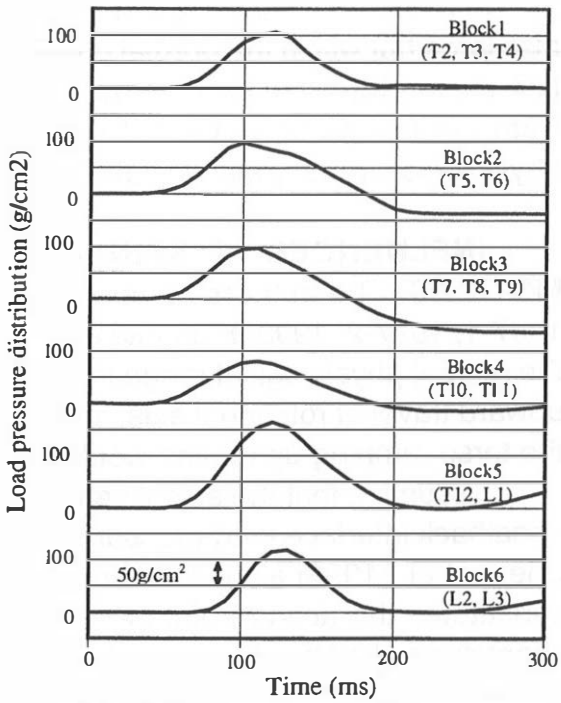


**Figure 24. Time-histories of interface pressure distribution divided into 6 blocks of sheet mat (The initial load is set to zero and curves are shown separately. Standard seat; 8 km/h)**

Table 4 shows an extract of combined flexion/extension data of thoracic and lumbar spines shown in a paper presented by Lumsden et al. (1968), White and Panjabi (1990). These data and those obtained in this study (Figures 18 and 23) are compared in the following. In case of rigid seat, the following were found: L3-L4: 7 degrees (flexion: F); T12-L1: 12 deg. (extension: E); T5-T6: 8 deg. (E), showing that the rotation angles of upper lumbar spines are large but within the normal physiological range, while those of thoracic spines (T4-T5 and T5-T6) are twice larger than the normal physiological values. In case of standard seat, on the other hand, the following were found: L2-L3: 8 degrees (E); L3-L4: 11 deg. (F); L4-L5: 9 deg. (F);

**Table 4. Limits and Representative Values of Ranges of Rotation**

| Interspace | Combined Flexion/Extension (+/- y-axis rotation) Limits of Ranges (degrees) | Repr sentative Angle (degrees) |
|---|---|---|
| Thoracic Spine | | |
| T1-T2 | 3-5 | 4 |
| T2-T3 | 3-5 | 4 |
| T3-T4 | 2-5 | 4 |
| T4-T5 | 3-5 | 4 |
| T5-T6 | 2-7 | 4 |
| T6-T7 | 3-8 | 5 |
| T7-T8 | 3-8 | 6 |
| T8-T9 | 3-8 | 6 |
| T9-T10 | 3-8 | 6 |
| T10-T11 | 4-14 | 9 |
| T11-T12 | 6-20 | 12 |
| T12-L1 | 6-20 | 12 |
| Lumbar Spine | | |
| L1-L2 | 5-16 | 12 |
| L2-L3 | 8-18 | 14 |
| L3-L4 | 6-17 | 13 |
| L4-L5 | 9-21 | 16 |
| L5-S1 | 10-24 | 17 |

T4-T5: 9 deg. (E), showing that the rotation angles of lower lumbar vertebrae are also large but within the normal physiological range, while those of thoracic spines (T4-T5) are twice larger than the normal physiological values. It can be deduced from the foregoing data that the upper thoracic spines moved beyond the physiological range, with its influence transmitted to the lower cervical vertebrae.

**INFLUENCES OF SPINAL MOTIONS ON CERVICAL VERTEBRAL MOTIONS** -The authors have suggested in an earlier study (Ono et al. 1993, 1997-1, 1997-2, 1998, Kaneoka et al. 1998) that cervical vertebrae would exceed the normal physiological range in rear impact, showing abnormal motion with the upward travel of rotational axis, and that the straightening of spinal vertebrae and the torso ramping-up motion would influence markedly.

Assuming that the spinal vertebrae are one flexible rod, the occupant's back - seatback interface load-pressure increases at some local regions upon contact. Shen, et al. (1998) also reported the localized force of seatback. The seatback constitutes the acting point of the force against the occupant's back, which is characterized by the concentration of the force mainly on the upper torso and the lumbar, though it may differ according to the seat stiffness. Shen, et al. (1998) analyzed the force, focusing mainly on the function of localized loading point but have not analyzed how the difference in loading point influences the occupant's head and neck. Furthermore, biomechanical experimental data regarding rear impact are not available, as pointed out by Kroonenberg, et al. (1997), and the validation of data is lagging.

The lumbar spinal motions are as follows. First, thighs travel backward with inertia during impact, then the pelvis (around S1-L5) interacts with the seatback, and the thigh motion turns into rotation against the pelvis. As a result, lumbar spines flex or extend. It may be said that the question of whether flexion or extension occurs depends on whether or not the pelvis sinks into the seat cushion - in other words, it depends on the seat cushion property.

Motions of the lower thoracic spines consist of the backward travel of the torso (T6-T8) with inertia, and the interaction between the torso and seatback resulting in the flexion or extension of the lower thoracic spines (T10-T12).

Motions of the upper thoracic spines are as follows. The head, neck and torso travel backward first with inertia by impact, then the shoulders including arms travel backward as the torso gets in contact with the seatback, followed by the backward extension of the head with inertia, resulting in the extension of the upper thoracic spines as the upper torso arches upward. At the same time, spinal vertebrae also extend. The pivotal region for the seatback force at this moment is near T6-T10.

It may be said that the foregoing results represent the mechanism of spinal straightening. That is, it can be deduced that the neck is pushed up due to the straightening of spinal vertebrae (lumbar and thoracic spines), and the motions of lower cervical vertebrae are transmitted to the upper cervical vertebrae, which may result in the impingement of synovial fold due to the upward travel of the instantaneous axis of rotation of the cervical vertebra.

Therefore, for the evaluation of seat properties aiming at the reduction of such neck injuries, it would be indispensable to develop proper anthropometric dummies and models with the human spine characteristics incorporated accordingly.

## CONCLUSION

In this study, spinal deformations of volunteers and seatback interface load-pressure distributions have been measured for the first time, in addition to the low speed rear impact experiments conducted on volunteers by means of cineradiography. The aim of this study was to verify the influences of seatback-torso interaction and the spine straightening on human cervical vertebral motions as described below.

1) In case of the rigid seat, the localized straightening of lumbar spines started around 30 ms after impact, and the localized straightening of thoracic spines occurred around 80 ms where the interaction between the seatback and the subject's shoulders became maximum.
2) With the standard seat, the pelvis started to sink around 70 ms, resulting in the localized straightening of the thoracic spine around 120 ms where the interaction between the seatback and the subject's shoulders became maximum.
3) For rigid seat, the rotation angles of the thoracic spines (T4-T5 and T5-T6) became about twice larger than the physiological range, although the rotation angles of the lower lumbar spines were roughly within the normal physiological range.
4) For standard seat, the rotation angles of the thoracic spines (T4-T5) exceeded the physiological range by two-folds, as in the case of rigid seat, although the rotation angles of the lower lumbar spines were roughly within the normal physiological range.
5) It can be deduced that such localized deformations of spines are likely to occur not only in the lumbar spines but also in the thoracic spines.

   The influences of seat stiffness on the localized spinal deformations are deduced as follows.
6) The question whether the lumbar spines flex or extend depends on how the pelvis and the thigh sink into the seat cushion - namely, it depends on the seat stiffness.
7) The localized extension of upper thoracic spines is caused by the backward travel of the shoulders including arms, as the torso interacts with the seatback by inertia, and the upper torso arches upward. In other words, it is important to control the upper torso motion properly.

It can be said according to the foregoing findings that it is vital to incorporate proper parameters - components of T1 translation and rotation which are necessary inputs related with the spinal straightening - in the analysis of cervical vertebrae.

## REFERENCES


Davidsson J., Ono K., Lovsund P., and Svensson M. : A Comparison between Volunteer and BioRID P3 Performance in Rear-End Sled Collisions Impacts, Proc. of IRCOBI Conference, in Press, 1999

Ishiyama S., Tsukada K., Nishigaki H., Ikeda Y., and Sakuma S.: Development of an Abdominal Deformation Measuring System for Hybrid III Dummy, 38th Stapp Car Crash ConferenceProceedings, SAE No. 942223, pp. 265-279, 1994

Kahane C. J.: An Evaluation of Head Restraints; Federal Motor Vehicle Safety Standard 202. NHTSA Technical Report DOT HS-806-108, February 1982

Kaneoka K. and Ono K.: Human Volunteer Studies on Whiplash Injury Mechanisms, "Frontiers in Head and Neck Trauma: Clinical and Biomechanical" , Publisher :IOS Press, Harvard, MA, 1998, pp. 313-325

Kroonenberg A., Thunnissen J., and Wismans J..: A Human Model for Low-severity Rear-Impacts, Proc. of IRCOBI Conference, Hannover, Germany, 1997, pp. 117-132

Lumsden R. M., and Morris J. M. : An In Vivo Study of Axial Rotation and Immobilization at the Lumbosacral Joint. J. Bone Joint Surg., 50 A:1591, 1968

Nygren A.: Injuries to Car Occupants. Some Aspects of Interior Safety of Cars - A Study of 5 years Material from an Insurance Company, Acta Otolaryngol Suppl (Stockholm) 1984 : (Suppl 395)

Ono K. and Kanno M.: Influences of the Physical Parameters on the Risk to Neck Injuries in Low Impact Speed Rear-end Collisions, Proceedings of the International IRCOBI Conference on the Biomechanics of Impact. Eindhoven, 1993: pp. 201-212.

Ono K, and Kaneoka K.: Motion Analysis of Human Cervical Vertebrae during Low Speed Rear Impacts By the Simulated Sled, Proc. of IRCOBI Conference, Hannover, Germany, 1997, pp. 223-237

Ono K., Kaneoka K., Wittek A., and Kajzer J.: Cervical Injury Mechanism Based on the Analysis of Human Cervical Vertebral Motion and Hed-Neck-Torso Kinematics During Low Speed Rear Impacts, Proc. of 41st Stapp Car Crash Conference SAE P-315, Paper No. 973340, Florida, Nov. 13-14, 1997, pp. 339-356

Ono K., Kaneoka K., and Inami S.: Influence of Seat Properties on Human Cervical Vertebral Motion and Head/Neck/Torso Kinematics During Rear-end Impacts, Proc. of IRCOBI Conference, Gothenberg, Sweden, 1998, pp. 303-318

Shen W., Wiklund K., Frid S., Swamy B., Nilson G., and Humer M.: Pressure and Load Patterns on Seat Interface: A Comparison between Human Subjects and Crash Test Dummies, Proc. of IRCOBI Conference, Gothenberg, Sweden, 1998, pp. 453-464

WHO/CIOMS Proposed Guidelines for Medical Research Involving Human Subjects, and the Guidelines on the Practice of Ethics Committees Published by the Royal College of Physicians, The Lancet, November 12, 1988, pp. 1128-1131

White III A. and Panjabi M.: Clinical Biomechanics of the Spine, Second Edition, Publisher : J. B. Lippincott Company, 1990. pp. 86-120